Appendix A: Research plan Axel Brandenburg (590407-8317)

1 Purpose and aims

Our Universe is well modeled by the theory of cold dark matter (CDM) with a non-vanishing integration constant, the Λ term in Einstein's equations, responsible for the accelerated expansion of the Universe over the past billion years. The *observational foundations* of the ΛCDM model rest upon three major pillars related to the epochs of Big Bang nuclear synthesis (when the Universe was ~ 15 minutes old), the cosmic microwave background (which formed when the universe was 400,000 years old), and the expansion history and large-scale structure of the Universe observed today. The major goal of this project is to help establishing a probe of the first microseconds of the Universe using magnetic fields and gravitational waves.

Primordial magnetic fields are routinely described in a diagnostic diagram of comoving field strength B versus comoving length scale λ_B; see Figure 1. Using the non-observation of extended and delayed secondary γ-ray emission from distant extragalactic sources such as active galactic nuclei (Neronov & Vovk, 2010; Acciari et al., 2023) and γ-ray bursts (Vovk et al., 2024), lower limits on B were previously obtained. Upper limits are now provided through residual rotation measures obtained from LOFAR Carretti et al. (2025).

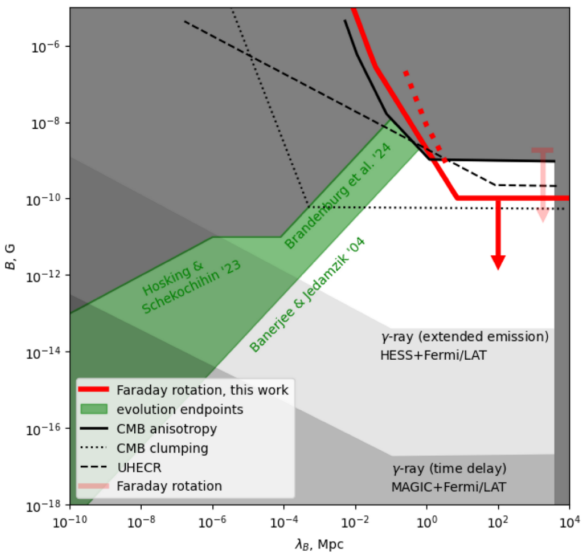

Figure 1: Primordial magnetic field limits B versus length scale λ_B obtained through the combination of radio and γ-ray observations of the low red shift universe, combined with advanced modeling of the evolution of magnetic fields with cosmic structures. Taken from Neronov et al. (2024).

Using numerical simulations, we will be able to use magnetic fields to trace back their origin to the epochs of inflation, or the electroweak (EW) or quark confinement (or QCD) phase transitions (PT). In addition, we will use the stochastic gravitational wave background to established a connection between the present day observed magnetic field and its possible source at one of the epochs in the early universe. Already now, pulsar timing array observations in the nHz range have traced their origin to the epoch of quark confinement (Brandenburg et al., 2021; Roper Pol et al., 2022). Higher frequencies in the mHz range will be available in future through Laser Interferometer Space Antenna (LISA).

Based on theory, we know that all magnetic field models have the endpoints on a unique line (Banerjee & Jedamzik, 2004; Hosking & Schekochihin, 2023; Brandenburg et al., 2024), although there are still some differences in their precise position; see Figure 1 from the work of Neronov et al. (2024). A particular point on this line has been identified by Jedamzik et al. (2025b), who showed that the Hubble tension (the 5σ discrepancy between the value of the Hubble constant of $67.36\,\mathrm{km/s\,kpc^{-1}}$ from Planck and $73.04\,\mathrm{km/s\,kpc^{-1}}$ from the SH0ES collaboration using type ia supernovae) can be alleviated by density enhancements caused by a primordial magnetic field of $5\,\mathrm{pG}$ at a scale of $\approx 1\,\mathrm{kpc}$. This is referred to as baryon clumping. A connection between the point $(B,\lambda_B)=(5\,\mathrm{pG},1\,\mathrm{kpc})$ of Jedamzik et al. (2025b) and the PTA data suggesting $(B,\lambda_B)=(1\,\mu\mathrm{G},0.1\,\mathrm{pc})$ can indeed be explained by a non-helical magnetic field evolution when $B\propto\lambda_B^{-5/4}$; see Hosking & Schekochihin (2023). This is shown

in Figure 2.

To be able to compute the amount of baron clumping at recombination and the field strength and coherence length today, we need to take into account the detailed ionization history and radiation dynamics at the time of photon decoupling from the matter, which occurs shortly before the epoch of recombination. As the photon mean-free path increases, the dissipation changes from a diffusion of particles at small mean-free path to a regime of drag from the free-streaming photon background. This leads to the magnetic field being frozen into the plasma. The overall purpose of this project is therefore:

- to study the magnetic field evolution near the time of photon decoupling,
- to assess the magnetic field level when it becomes frozen into the plasma, and
- to compute the effects of the magnetic field on the cosmological evolution.

The latter topic is crucial for addressing the Hubble tension and other discrepancies between the late and early evolution of the Universe; see Jedamzik & Pogosian (2020) and Jedamzik et al. (2025a).

A major realization of the last few years was the discovery of what is now called the Hosking integral, a new conserved quantity. It is the correlation integral of the magnetic helicity variance and governs magnetically dominated turbulence in previously unknown and surprising ways. The basic idea is that magnetic helicity, while it may be vanishing on average, it is always finite in patches. The relevant conserved quantity is the Hosking integral (Hosking & Schekochihin, 2021). As already alluded to in the beginning, their subsequent work (Hosking & Schekochihin, 2023) also makes another remarkable claim, namely that the overall decay time τ of the magnetic energy density is not only governed by the decay exponent, but also by the timescale, which, if expressed in terms of the instantaneous Alfvén time $\tau_{\rm A}$, depends on the microphysical magnetic resistivity. This is quantified by the coefficient $C_{\rm M}$ in the relation $\tau = C_{\rm M}\tau_{\rm A}$. From a hydrodynamic point of view (no magnetic fields), this would be unexpected, because hydrodynamic turbulence is known to be independent of the microphysical viscosity. This is a basic assumption underlying the applicability of large eddy simulations, which may thus not be correct in the presence of strong magnetic fields.

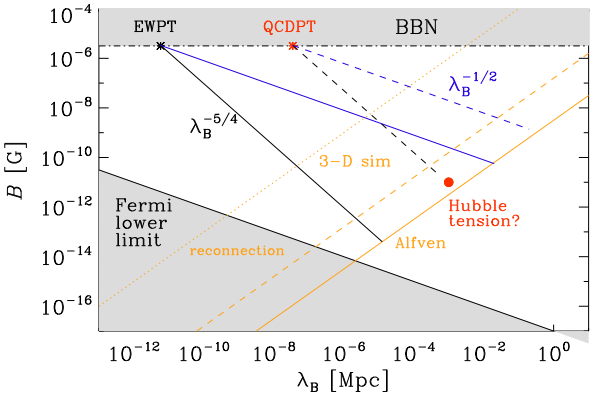

Figure 2: Decay of a nonhelical magnetic field $B \propto t^{-5/9}$ with conformal time t and growth of the magnetic length scale $\lambda_B \propto t^{4/9}$ corresponds to an evolution $B \propto \lambda_B^{-5/4}$ in a diagram showing B versus λ_lambda_B (black lines). The asterisks denote the start of the evolution from the electroweak phase transition (EWPT, black) or the QCD phase transition (QCDPT, red), with the maximally allowed value for B to not affect the rate of neutron β-decay, which would affect the ^{4}He abundance during big bang nucleosynthesis (BBN). The evolution stops at one of the orange lines; which one is subject to the present proposal. The solid line corresponds to Alfvén scaling (assumed in Banerjee & Jedamzik, 2004), the dotted line applies if the decay is constrained by reconnection with a large magnetic Prandtl number (assumed in Hosking & Schekochihin, 2023). The dashed line is the result of preliminary numerical investigations in 2-D (Brandenburg et al., 2024). The blue line corresponds to helical decay. The red point marked with 'Hubble tension?' refers to what might be needed to alleviate it.

In magnetohydrodynamics (MHD), the strength of a turbulent magnetic field with a root-mean-square (rms) magnetic field $B_{\rm rms}$ is characterized by the Alfvén speed, $v_{\rm A} = B_{\rm rms}/\sqrt{\mu_0\rho_0}$, where μ_0 is the permeability and ρ_0 is the density. The resistivity or magnetic diffusivity η is then quantified by the Lundquist number ${\rm Lu} = v_{\rm A}/\eta k_0$, where k_0 is the peak wavenumber of the magnetic energy spectrum. Our preliminary work confirms a resistive dependence of the decay time, but leaves important questions still answered. Can we trust the numerics,

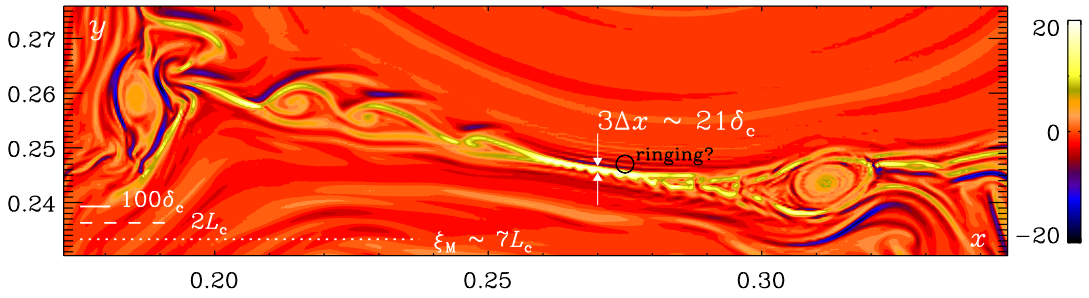

Figure 3: Zoom-in of a small piece of a 2-D simulation of decaying MHD turbulence showing a current sheet (yellow) breaking up into little islands (plasmoids). Yellow (blue) tones correspond to positive (negative) values of the normal component of the current density in a simulations with $\mathrm{Pr}_M = 10$ using 16384^2 mesh points over $(2\pi)^2$. The lengths of $100\,\delta_{\rm c}$, $2L_{\rm c}$, and λ_B are indicated by horizontal white solid, dashed, and dotted lines, respectively. The thickness of the current sheet corresponds to about $3\Delta x \approx 21\,\delta_{\rm c}$, where Δx is the mesh spacing. In its proximity, there are also indications of ringing, indicated by the black circle. Adapted from Brandenburg et al. (2024).

especially when the magnetic Prandtl number (Pr_M, i.e., the ratio of microphysical viscosity to microphysical magnetic diffusivity) is large? A Pr_M-dependence is found in driven magnetic reconnection (Comisso et al., 2015), where a single current sheet of length $L_{\rm c}$ and thickness $\delta_{\rm c}$ is seen to break up into smaller ones due to the production of plasmoids. In our 2-D simulations of turbulent decay, we also see plasmoid production; see Figure 3.

But reconnection is an idealized experimental setup that may not have much to say about turbulence. In particular, in decaying turbulence simulations, reconnection sites are intermittent in time and space and are not volume-filling, so their role may not be very important. We will therefore carry out carefully designed control experiments, focusing on possible artifacts from finite domain sizes. Earlier work of Hosking & Schekochihin (2021) has claimed to be able to take advantage of using hyperviscosity and hyperresistivity, but there are concerns about side effects. It is therefore important to reconsider the possibility of artifacts. Here, we will instead perform full radiation-hydrodynamic simulations.

Around the epoch of recommendation, i.e., near the end of the radiation dominated era, the photon mean-free path becomes very long and introduces damping of the velocity field. This effect has been examined in earlier work (Banerjee & Jedamzik, 2004; Hosking & Schekochihin, 2023), but this was only done in an approximate way. Here, we will produce very large resolution simulations where we introduce and study this effect on the decay law. Simulations with coupling to the photon field are also important for alleviating the Hubble tension by lowering the sound horizon through magnetically produced density clumping (Jedamzik & Pogosian, 2020; Jedamzik et al., 2025a).

An important aspect of all future simulation is the utilization of graphics processing units (GPUs). For that purpose, we will also utilize the Large Unified Modern Infrastructure LUMI in Kajaani (Finland); see Pekkilä et al. (2022) for relevant code development relevant for the PENCIL CODE (Pencil Code Collaboration, 2021). In summary, to accomplish the goals outlined in this proposal, our specific aims are as follows.

- Determine the scaling of MHD turbulence decay with Lundquist and magnetic Prandtl numbers. Assess artifacts resulting from finite domain size and finite resolution.
- Is there evidence for a saturation of the Lundquist number dependence of $C_{\rm M}$ in 3-D? This has so far only been seen in 2-D simulations, so new high-resolution 3-D simulations at 8192^3 mesh points may already suffice to demonstrate the saturation in 3-D simulations. Compare 3-D with

2-D and 2.5-D simulations, where the magnetic field has a component out of the plane.

- Is it true that $C_{\rm M}$ is independent of ${\rm Pr}_M$? How does the answer to this question depend on numerical aspects such as the resolution, the range of ${\rm Pr}_M$, i.e., can we expect and see a dependence already in the range 1–10, or do we need to go to the range 10–100, or even larger?
- What is the physics of the Lundquist number dependence at small values of Lu and of the saturation phenomenon? Is it related to the physics of reconnection? But if so, why is there no dependence of $C_{\rm M}$ on ${\rm Pr}_M$, if it is indeed true that there is no such ${\rm Pr}_M$-dependence in the decay of magnetic turbulence?
- Are there differences to forced reconnection experiments, where a dependence on ${\rm Pr}_M$ has been obtained (Comisso et al., 2015) and tentatively been reproduced (our preliminary work)?
- Consider the effects of radiative damping, which is relevant to the time of recombination. Check numerical restrictions regarding the number of rays and the efficiency of correction factors that were found to be useful in radiative cooling calculations in 2–D.
- Compared to earlier approximate treatments in terms of photon viscosity in the optically thick regime, and photon drag in the free-streaming regime, how important is a proper treatment of radiation to describe the effect of photon damping near the epoch of recombination? Is its functional form analogous to that of radiative cooling (Barekat & Brandenburg, 2014), where we know the answer and have included it routinely in simulations?

All these aims are compatible with past research experience of the PI, as demonstrated by his papers, especially in the last few years.

2 State of the art

In a recent paper (Brandenburg et al., 2024), we have computed the decay and Alfvén times as $\tau = (\mathrm{d}\ln v_{\rm A}^2/\mathrm{d}t)^{-1}$ and $\tau_{\rm A} = \lambda_B/v_{\rm A}$, and related them through $\tau = C_{\rm M}\tau_{\rm A}$. Here, λ_B is the integral scale of the turbulence, i.e., the inverse wavenumber of the peak of the spectrum, and $v_{\rm A}$ is the Alfvén speed. Our 3-D data points show an increase of $C_{\rm M}$ with Lu for small values of Lu. The $C_{\rm M}$ dependence on Lu is qualitatively similar for 2–D and 3–D turbulence. Moreover, the 2–D data points show that it becomes shallower for larger values of Lu. There is now evidence for $C_{\rm M}$ to level off and to become independent of Lu.

Reconnection has been studied for a very long time starting with the seminal works of Sweet and Parker, and then Petschek in the 1950s and 1960s. Much of our knowledge is derived from 2-D simulations. We know, for example, that current sheets develop that have a length $L_{\rm c} = {\rm Lu}_{\rm crit}\,\eta/v_{\rm A}$, where ${\rm Lu}_{\rm crit}$ is the critical value of the Lundquist number above which the plasmoid instability sets in, and $\delta_{\rm c} = L_{\rm c}/{\rm Lu}_{\rm c}^{1/2}$ is its thickness (Uzdensky, 2010). However, the possible connection to the decay of MHD turbulence is not at all obvious. A priori, one might have thought that, analogously to hydrodynamic turbulence, the decay time τ is just given by the dynamic or Alfvén time scale $\tau_{\rm A} = \lambda_B/v_{\rm A}$. This was assumed in the work of Banerjee & Jedamzik (2004). However, it now turns out that this is indeed too naive and now we know that τ and $\tau_{\rm A}$ are related to each other through a prefactor, i.e., $\tau = C_{\rm M}\tau_{\rm A}$. This was suggested based on analogies with reconnection; see Hosking & Schekochihin (2023) for the details of this idea. An alternative idea is that the slow-down of the turbulent decay is related to magnetic helicity conservation. Here, we have to remember that the idea of the Hosking integral is, again, that magnetic helicity is conserved, but now only in smaller subvolumes. Thus, it is reasonable to expect a connection between the two.

At the end of photon decoupling, our simulations automatically produce density inhomogeneities. This has previously been studied separately, where the resulting baryon clumping enhances the recombination rate. This results in an earlier recombination and a subsequent reduction of the size of the cosmic sound horizon. This, in turn, alters the positions of the peaks of the cosmic microwave background (CMB) temperature spectrum and changes the estimate of the expansion rate of the Universe, given by the Hubble parameter H_0 from CMB data (Jedamzik & Pogosian, 2020; Jedamzik et al., 2021). This is particularly relevant in the context of one of the hottest topics in cosmology nowadays, i.e., the tension between the measurements of H_0 from CMB and low-redshift probes (Di Valentino et al., 2021; Kamionkowski & Riess, 2022). Accounting for magnetically-induced baryonic clumping may alleviate this tension (Jedamzik & Pogosian, 2020; Galli et al., 2022). The Hubble tension could thus hint at the presence of a primordial magnetic field during recombination. Our models may provide a self-consistent description of the coevolution of magnetic fields with the primordial plasma, to test the presence of a magnetic field at recombination and its influence on the CMB observables.

As with most observed phenomena in astrophysics, there can be multiple explanations that need to be kept in mind. Regarding the Hubble tension, another important contender—also studied at Nordita—is the idea that the sound horizon is lowered by the injection of energy from a phase transition in the dark sector Niedermann & Sloth (2021). Regarding intergalactic magnetism, an important contender is outflows (Aramburo-Garcia et al., 2022). However, recent work by Tjemsland et al. (2024) shows that their filling factors are likely insufficient to explain the observations. Finally, regarding the stochastic gravitational wave background, other known sources include supermassive black hole mergers; see, e.g., Burke-Spolaor et al. (2019). We will therefore keep an open mind and follow the latest literature.

3 Significance and scientific novelty

The length scales of magnetic fields produced at the electroweak phase transition would be extremely small. Turbulence, however, changes this picture because of the possibility of an inverse cascade (Brandenburg et al., 1996). In recent years, this topic has gained tremendous attention. This is connected with the observational impact both for the contemporary universe to interpret the lower magnetic field limits, and the early universe, where relic gravitational waves could be an important messenger. With our simulations, we will prepare the ground for probing physics of the first microseconds of the Universe, when important processes occurred, e.g., the development of the matter–antimatter asymmetry.

Over the last two decades, it has become clear that in astrophysics, the concept of Kolmogorov turbulence must be superseded by one involving magnetic fields. This is because in all astrophysical plasmas, magnetic fields strongly interact with turbulent flows. This leads to dynamo action, which is now understood to be unavoidable, i.e., dynamos always operate under turbulent conditions, which are ubiquitous. The significance of the Hosking integral is that it governs the evolution in many of these generic cases were magnetic helicity vanishes on average, but still plays a role locally. This concept is much broader than originally imagined: it also applies to neutrons star crusts (Brandenburg, 2020), to relativistic plasmas with fermion chirality canceling magnetic helicity (Brandenburg et al., 2023a), and to the decay of MHD turbulence with arbitrary initial spectra (Brandenburg et al., 2023b). There may be many more.

We envisage that the next decade will see a shift from simulations where the microphysics is captured entirely by numerical schemes to simulations with more realistic prescriptions of the microphysics. Standard Spitzer resistivity only applies to collisional plasmas. In collisionless plasmas, dissipation is governed by instabilities, which affect the cascade in nonlocal ways that might need to be incorporated. Recent work by Meyrand et al. (2019) shows that this can still be done in a fluid description.

We also envisage an increasing role played by magnetic helicity, both globally on average, and also

locally within magnetic patches. We simulate this with the PENCIL CODE (Pencil Code Collaboration, 2021). However, many other codes do not use the magnetic vector potential. This has hampered the understanding of magnetic helicity in astrophysical plasmas, such as in the Sun, galaxies, and accretion discs.

4 Preliminary and previous results

The idea that $C_{\rm M}$ versus Lu saturates near $\mathrm{Lu_c} = 2.5 \times 10^4$ is solely motivated by 2–D simulations and the proximity between the 2–D and 3–D results. This may not be very safe in view of the fact that there are systematic differences is between the two. While we see inverse cascading in both cases, the envelopes of the spectral magnetic peaks are different: $\propto k^{3/2}$ in 3–D, and $\propto k$ in 2–D. This has to do with the different conservation laws: the Hosking integral 3–D and the anastrophy (i.e., $\langle A_z^2 \rangle$) in 2–D; see Brandenburg et al. (2024) for details. Thus, while our results are interesting, they may still not provide a useful answer.

In MHD, one sometimes talks about 2.5 dimensional magnetic fields. Those are still two-dimensional in the sense that $\boldsymbol{B} = \boldsymbol{B}(x, y)$, but all three components may be finite. By contrast, in 2–D (in the restricted sense) one means a field $\boldsymbol{B}_\perp = \boldsymbol{\nabla} \times (\hat{\boldsymbol{z}} A_z) = (\partial_y A_z, -\partial_x A_z, 0)$. Such fields have zero magnetic helicity pointwise, so also the Hosking integral vanishes, but in 2.5–D, the Hosking integral is finite, and then the anastrophy is no longer conserved. As a test, we envisage (and will check) that $\langle \boldsymbol{B}_\perp^2 \rangle$ decays like $t^{-10/9}$, while $\langle B_z^2 \rangle$ should decay like t^{-1}. Whether 2.5–D simulations provide useful intermediate step for understanding turbulence in early universe needs to be checked carefully.

So far, only the groups using the PENCIL CODE and SNOOPY have been calculating magnetic helicity evolution and fluxes in their simulations. Furthermore, most other codes only have implicit dissipation, so a value of Lu cannot be defined unambiguously. It is therefore important to compute the actual dissipation, especially that of small-scale magnetic helicity. In Brandenburg & Scannapieco (2020), we have shown that the eight-wave MHD solver in the `FLASH` code suffers from artifacts in the magnetic helicity evolution. We expect and are therefore exploring the potential artifacts that emerge in such codes.

5 Project description

5.1 Theory and method

To model the evolution of the magnetic field after its generation during the radiation-dominated era, we perform very high resolution simulations of decaying turbulence and determine the decay rate in terms of the Alfvén time over a range of Lundquist and magnetic Prandtl numbers. These numbers characterize the resistivity and viscosity. One of the difficulties is to assess artifacts resulting from making compromises by choosing the position of the peak of the spectrum neither too close to the smallest wavenumber of the computational domain nor too close to the largest one, in which case the inertial range of the turbulence would not be large enough. Additional compromises can be made by invoking hyperviscosity and hyperresistivity. These tools tend to shorten the dissipation range and prolong the inertial range, but they also modify the problem in ways that may not yet be fully understood. Therefore, we will perform systematic studies of the dependence on all the secondary input parameters (scale separation toward $k \ll k_0$ and $k \gg k_0$, as well as the order of the diffusion operator in cases with hyperdiffusion).

By calculating the magnetically induced effect on density, we can assess the role of clumping and whether this significantly changes the sound horizon and thereby the effect on the Hubble tension (Jedamzik et al., 2025a). Specifically, we plan to determine the contrast of density structures that are

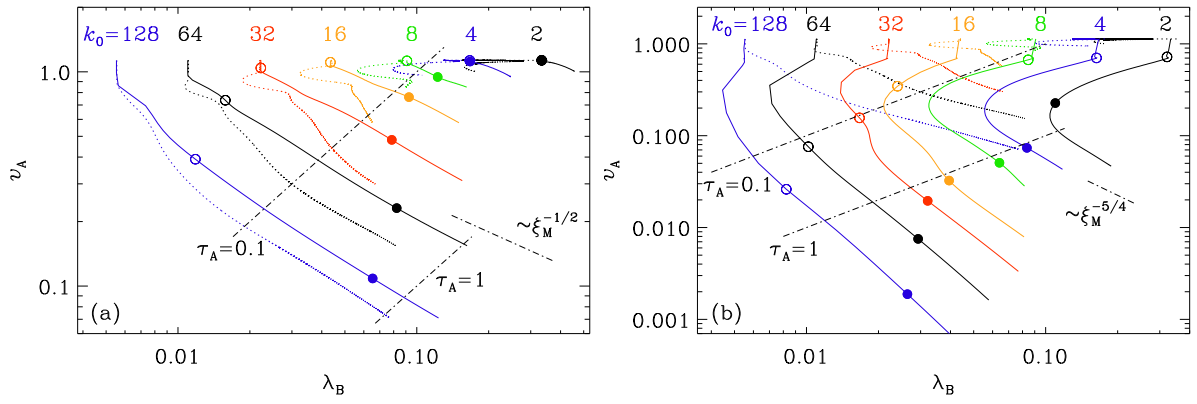

Figure 4: Parametric representation of $v_{\rm A}=B_{\rm rms}/\sqrt{\rho\mu_0}$ versus λ_B for helical (left) and nonhelical (right) initially columnar fields of different scale characterized by the fractional wavenumber $k_0=2$ (black), 4 (blue), 8 (green), and 16 (orange), 32 (red), 64 (black), and 128 (blue). The open (filled) symbols in both plots indicate the times $t=10$ ($t=100$). Adapted from Brandenburg et al. (2025).

caused by the magnetic field at the end of the radiation-dominated era. We also need to assess the damping caused by the photon fluid on the velocity field. This could shorten the decay time expressed in terms of the Alfvén time. These density fluctuations will also affect the resulting Biermann battery effect discussed in earlier work of Naoz & Narayan (2013) as alternative to earlier magnetogenesis scenarios.

Given that the correlation length $\lambda_B(t)$ and magnetic energy density $\mathcal{E}_{\rm M}(t)$ are power laws in time, it was thought that the values at time t,

$$\lambda_B(t)=\lambda_{B0}\left(\frac{t}{t_0}\right)^{\frac{4}{9}},\ \mathcal{E}_{\rm M}(t)=\mathcal{E}_{\rm M0}\left(\frac{t}{t_0}\right)^{-\frac{10}{9}} \tag{1}$$

depend on *two* adjustable parameters: $\lambda_{B0}\equiv\lambda_B(t_0)$ and $\mathcal{E}_{\rm M0}\equiv\mathcal{E}_{\rm M}(t_0)$, but we now know that the correct expression leaves less freedom (Brandenburg & Larsson, 2023; Brandenburg & Banerjee, 2025; Vachaspati, & Brandenburg, 2025)

$$\lambda_B(t)=C_{\rm H}^{\lambda}I_{\rm H}^{1/9}t^{4/9},\quad \mathcal{E}_{\rm M}(t)=C_{\rm H}^{\mathcal{E}}I_{\rm H}^{2/9}t^{-10/9}, \tag{2}$$

and depends only on *one* parameter, the conserved quantity $I_{\rm H}$, if it is indeed true that $C_{\rm H}^{\lambda}\approx0.14$ and $C_{\rm H}^{\mathcal{E}}\approx4.0$ are *universal* parameters. However, at least in the non-helical case, the evolution does not always start off as a straight power law; see Figure 4 where we compare helical (left) and non-helical cases (right) for two special initial conditions. Here the initial fields are columnar, which is motivated by what can be realized in a plasma experiment.

The theory of non-helical turbulent decay is not (yet) universally accepted, and some simulations yield different results (Armua et al., 2023; Dwivedi et al., 2024). Reasons include the occurrence of artifacts related to the to finite scale separation, or the use of hyperviscosity or time dependent, viscosity, or the slow-limited diffusion scheme used in some simulations. In the PENCIL CODE, we can test all these scenarios and compare with direct numerical simulations, where no such tools are employed.

5.2 Time plan and implementation

We begin by assessing the artifacts resulting from the use of hyperviscosity and hyper-resistivity, the finite domain size, and dependence on the aspect ratio of the computational domain. These calculations

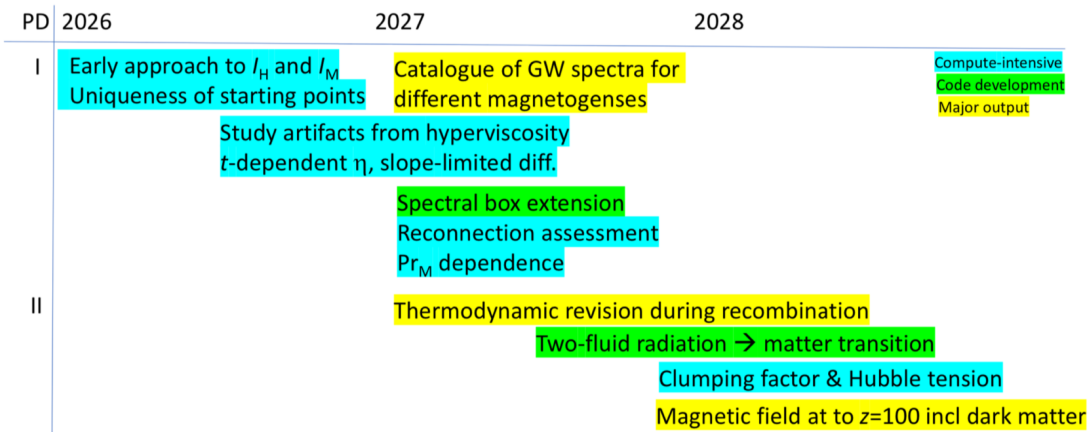

Figure 5: Time line of the project and tasks of PDs I and II. Compute-intensive and code development tasks are highlighted in blue and green, respectively, while major outputs are in yellow.

will help us assessing the quality of a new technique to a propagate inversely cascading turbulence to larger domains as time goes on. Here we will employ a technique called spectral box extension, which can be performed in two ways: (i) by simply re-initializing a simulation from previously computed energy spectra by randomizing the phases in Fourier space, or (ii) by supplying random modes at the smallest wavenumbers only. This technique will need to be implemented into the PENCIL CODE and requires some code development. At the end of our exploration of different magnetogenesis scenarios, we will have a catalogue of new models of magnetic fields and their associated gravitational wave data that constitute a major output of our project. All this will be done together with a postdoc; see the timeline in Figure 5.

During the second year, the postdoc will focus on all aspects related to understanding the magnetic field evolution at the transition from radiation to matter domination. I have started doing some exploratory calculations with the PENCIL CODE using the hydrogen ionization module. During recombination, many thermodynamic functions such as the specific heats at constant pressure and volume (c_p and c_v) and factors related to latent heat effects very significantly; see Figure 6. Such variations have been neglected in the work of Jedamzik et al. (2025a), so one of our major outputs will be the establishment of such thermodynamic variations and their effect on baryon clumping.

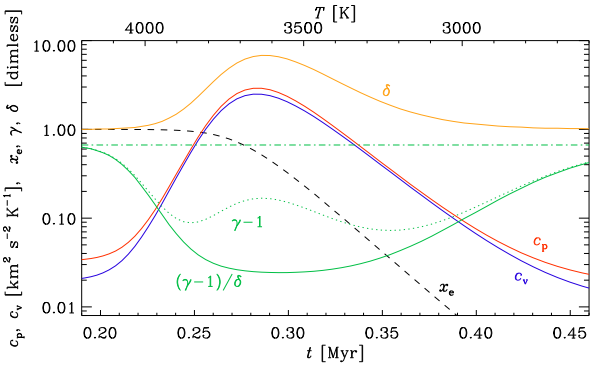

Figure 6: Dependences of c_p and c_v, as well as $\gamma = c_p/c_v$, the ionization fraction x_e, and $\alpha = (\partial \ln \rho / \partial \ln p)_T$, which enters in the expression for the sound speed $c_s = \sqrt{\gamma p/\rho\alpha}$, where p is pressure.

To model the transition to matter domination, Jedamzik et al. (2025a) initiated the simulations in a completely matter-dominated gas. While we may also do this with the PENCIL CODE, we plan to exploit a two-fluid framework in which the photon gas that was simulated in radiation domination is also included and coupled to the matter fluid. This also requires some code development.

Both with single and two-fluid models, we will compute the clumping factor that governs the reduction of the sound horizon at the time of recombination, which thereby contributes to alleviating the

Hubble tension. This will be another compute-intensive step. As a major deliverable, our work will then produce magnetic field snapshots that also include the early dark matter evolution, which can be then be used in realistic ΛCDM models of the low red shift Universe; see, e.g., joint work with Mtchedlidze (2024).

Mile stones. We monitor the progress through the achievement of the following mile stones.

- Conclusive assessment regarding the artifacts and advantages of using hyperviscosity and hyperresistivity, the finite domain size effects, as well as dependence on the aspect ratio of the computational domain (during 2026).
- Catalogue of magnetic field and gravitational wave data from a range of magnetogenesis models (during 2027).
- New models with the spectral box extension (during 2027).
- Conclusive assessment regarding the magnetically produced baryon clumping and the effect of variations of thermodynamic properties during recombination (during 2028).
- Snapshots of magnetic field, density, and velocity at $z = 100$ with proper early dark matter evolution (during 2028).

Risks. Spectral box extension has so far only been used by simply re-initializing a simulation from previously computed energy spectra by randomizing the phases in Fourier space. If the technique of supplying random modes at the smallest wavenumbers only turns out to be problematic, the initializing from spectra is a fall-back option. It is also not clear whether the two-fluid framework with photon gas coupled to the matter fluid is needed. A fall-back option is to model only the transition to matter domination, as done by Jedamzik et al. (2025a). Another risk is to lose local in-house expertise in high-performance computing. This increases the demand on us for hands-on help in computing. Already now, we mitigate this by monthly PENCIL CODE office hours and disseminating information through the PENCIL CODE newsletter.

Backup plan. In addition to the risk mitigations addressed above, there are several alternative routes if the need emerges.

- The study of artifacts may not be conclusive. We should then attempt to provide tighter error margins on the scaling coefficients.
- Radiation may limit the time step prohibitively. We can then artificially lower the radiation field and study the scaling of the final results with this reduction.
- Alternative explanations for Hubble tension, intergalactic magnetic fields, or the stochastic gravitational wave background may gain increased attention. This would open many possibilities for backup studies if other aspects of our project become problematic.

5.3 Project organization

At Nordita, most of my time is devoted to research. I am therefore able to spend at least 60% of my time on this project, which includes the supervision of the postdocs to be supported on this project. A committee will be set up to select the postdoc with the best competences (physical insight, numerical proficiency, etc). Experience with turbulence and ΛCDM cosmology will be advantageous.

6 Equipment & Need for research infrastructure

This project utilizes national supercomputing resources through the National Academic Infrastructure for Supercomputing in Sweden (NAISS), which also provides resources on GPU cluster LUMI in Finland. National supercomputing resources have been used routinely by the PI. We are currently using 1.5 million CPU hours per month at PDC in Stockholm and a smaller amount at NSC in Linköping. We also hold an allocation of 2.6 million CPU hours and 248 000 GPU hours on LUMI. This is usually sufficient to cover our regular needs for most of our production runs. In the event of very large computing needs, we plan to apply for European PRACE resources.

7 International and national collaboration

I enjoy a large network of international collaborators. Particularly important for this project is my collaboration with Chiara Caprini (Geneva), Andrii Neronov (Paris & Lausanne), and Franco Vazza (Bologna), as well as with Tina Kahniashvili (Carnegie Mellon U), Evangelos Sfakianakis (Case Western Reserve U), and Oksana Iarygina (Marie-Curie fellow at Nordita). There is also the community of PENCIL CODE users, and we meet annually during in-person PENCIL CODE User Meetings and monthly during office hours via zoom. During conferences in general, new collaborations have emerged spontaneously, as evidenced by the list of publications of the PI with new collaborations in recent years.

8 Independent line of research

As is evident from my CV, I have been managing small research groups during my entire career.

References

Acciari, V. A., Agudo, I., Aniello, T., et al. 2023, A&A, 670, A145
Aramburo-Garcia, A., Bondarenko, K., Boyarsky, A., et al. 2022, MNRAS, 515, 5673
Armua, A., Berera, A. & Calderón-Figueroa, J. 2023, PRE, 107, 055206
Banerjee, R., & Jedamzik, K. 2004, PRD, 70, 123003
Barekat, A., & Brandenburg, A. 2014, A&A, 571, A68
Brandenburg, A. 2020, ApJ, 901, 18
Brandenburg, A., & Banerjee, A. 2025, J. Plasma Phys., 91, E5
Brandenburg, A., & Larsson, G. 2023, Atmosphere, 14, 932
Brandenburg, A., Enqvist, K., & Olesen, P. 1996, PRD, 54, 1291
Brandenburg, A., Clarke, E., He, Y., & Kahniashvili, T. 2021, PRD, 104, 043513
Brandenburg, A., Neronov, A., & Vazza, F. 2024, A&A, 687, A186
Brandenburg, A., Yi, L., & Wu, X. 2025, arXiv:2501.12200
Brandenburg, A., & Scannapieco, E. 2020, ApJ, 889, 55
Brandenburg, A., Kamada, K., & Schober, J. 2023a, PRR, 5, L022028
Brandenburg, A., Sharma, R., & Vachaspati, T. 2023b, J. Plasma Phys., 89, 905890606
Burke-Spolaor, S., et al. 2019, A&A Rev., 27, 5
Carretti, E., Vazza, F., O'Sullivan, S. P., et al. 2025, A&A, 693, A208
Comisso, L., Grasso, D., & Waelbroeck, F. L. 2015, Phys. Plasmas, 22, 042109
Di Valentino, E., et al. 2021, Class. Quant. Grav, 38, 153001
Dwivedi, S., Anandavijayan, C., & Bhat, P. 2024, Open J. Astrophys., 7, 75
Galli, S., Pogosian, L., Jedamzik, K., & Balkenhol, L. 2022, PRD, 105, 023513
Hosking, D. N., & Schekochihin, A. A. 2021, PRX, 11, 041005
Hosking, D. N., & Schekochihin, A. A. 2023, Nat. Comm., 14, 7523
Jedamzik, K., & Pogosian, L. 2020, Phys. Rev. Lett., 125, 181302
Jedamzik, K., Abel, T., & Ali-Haïmoud, Y. 2025a, J. Cosm. Astrop. Phys., 03, 12
Jedamzik, K., Pogosian, L., & Abel, T. 2025b, arXiv:2503.09599
Jedamzik, K., Pogosian, L., & Zhao, G.-B. 2021, Comm. Phys., 4, 123
Kamionkowski, M., & Riess, A. G. 2022, ARNPS, 73, 153
Meyrand, R., Kanekar, A., Dorland, W., & Schekochihin, A. A. 2019, Proc. Nat. Acad. Sci., 116, 1185
Mtchedlidze, S., Domínguez-Fernández, P., Du, X., Carretti, E., Vazza, F., O'Sullivan, S. P., Brandenburg, A., & Kahniashvili, T. 2024, ApJ, 977, 128
Naoz, S., & Narayan, R. 2013, Phys. Rev. Lett., 111, 051303
Neronov, A., & Vovk, I. 2010, Science, 328, 73
Neronov, A., Vazza, F., Mtchedlidze, S., & Carretti, E. 2024, arXiv:2412.14825
Niedermann, F., Sloth, M. S. 2021, PRD, 103, L041303 New early dark energy
Roper Pol, A., Caprini, C., Neronov, A., & Semikoz, D. 2022, PRD, 105, 123502
Pekkilä, J., Väisälä, M. S., Käpylä, M. J., Rheinhardt, M., & Lappi, O. 2022, Parallel Comp., 111, 102904
Pencil Code Collaboration 2021, J. Open Source Softw., 6, 2807
Tjemsland, J., Meyer, M., & Vazza, F. 2024, ApJ, 963, 135
Uzdensky, D. A., Loureiro, N. F., & Schekochihin, A. A. 2010, Phys. Rev. Lett., 105, 235002
Vachaspati, T., & Brandenburg, A. 2025, PRD, 111, 043541
Vovk, I., Korochkin, A., Neronov, A., & Semikoz, D. 2024, A&A, 683, A25